SARS-CoV-2 variants of concern remain dependent on IFITM2 for efficient replication in human lung cells

Rayhane Nchioua[1], Annika Schundner[2], Dorota Kmiec[1], Caterina Prelli-Bozzo[1], Fabian Zech[1], Lennart Koepke[1], Alexander Graf[3], Stefan Krebs[3], Helmut Blum[3], Manfred Frick[2], Konstantin M. J. Sparrer[1], and Frank Kirchhoff[1#]

[1] Institute of Molecular Virology
Ulm University Medical Center
89081 Ulm, Germany

[2] Institute of General Physiology
Ulm University Medical Center
89081 Ulm, Germany

[3] Laboratory for Functional Genome Analysis
Gene Center, LMU München,
80539 Munich, Germany

[#] address correspondence to:
Frank Kirchhoff
Phone: 49-731-50065150
Fax: 49-731-50065153
frank.kirchhoff@uni-ulm.de

Running title: IFITM dependency of SARS-CoV-2 VOCs

29 **ABSTRACT**

30 **It has recently been shown that an early SARS-CoV-2 isolate (NL-02-2020) hijacks**
31 **interferon-induced transmembrane proteins (IFITMs) for efficient replication in human**
32 **cells. To date, several "Variants of Concern" (VOCs) showing increased infectivity and**
33 **resistance to neutralization have emerged and globally replaced the early viral strains.**
34 **Here, we determined whether the four SARS-CoV-2 VOCs (Alpha, Beta, Gamma and**
35 **Delta) maintained the dependency on IFITM proteins for efficient replication. We found**
36 **that depletion of IFITM2 strongly reduces viral RNA production by all four VOCs in the**
37 **human epithelial lung cancer cell line Calu-3. Silencing of IFITM1 had little effect, while**
38 **knock-down of IFITM3 resulted in an intermediate phenotype. Strikingly, depletion of**
39 **IFITM2 generally reduced infectious virus production by more than four orders of**
40 **magnitude. In addition, an antibody directed against the N-terminus of IFITM2 inhibited**
41 **SARS-CoV-2 VOC replication in iPSC-derived alveolar epithelial type II cells thought to**
42 **represent major viral target cells in the lung. In conclusion, endogenously expressed IFITM**
43 **proteins (especially IFITM2) are critical cofactors for efficient replication of genuine**
44 **SARS-CoV-2 VOCs, including the currently dominating Delta variant.**

45 **IMPORTANCE**

46 Recent results showed that an early SARS-CoV-2 isolate requires endogenously expressed
47 IFITM proteins for efficient infection. However, whether IFITMs are also important cofactors
48 for infection of emerging SARS-CoV-2 VOCs that out-competed the original strains and
49 currently dominate the pandemic remained to be determined. Here, we demonstrate that
50 depletion of endogenous IFITM2 expression almost entirely prevents the production of
51 infectious Alpha, Beta, Gamma and Delta VOC SARS-CoV-2 virions in a human lung cell line.
52 In comparison, silencing of IFITM1 had little impact, while knock-down of IFITM3 had
53 intermediate effects on viral replication. Finally, an antibody targeting the N-terminus of IFITM2
54 inhibited SARS-CoV-2 VOC replication in iPSC-derived alveolar epithelial type II cells. Our
55 results show that SARS-CoV-2 VOCs including the currently dominant Delta variant are
56 dependent on IFITM2 for efficient replication suggesting that IFITM proteins play a key role in
57 viral transmission and pathogenicity.

58 **INTRODUCTION**

59 Since its first occurrence in Wuhan (China) in December 2019, the severe acute respiratory
60 syndrome coronavirus 2 (SARS-CoV-2), the causative agent of coronavirus disease 2019
61 (COVID-19), has caused a devastating pandemic (1, 2). The reasons for the efficient spread of
62 this coronavirus are not fully understood but clearly involve the ability to efficiently infect and
63 propagate in human cells. Viral entry depends on binding of the viral Spike (S) protein to the
64 cellular angiotensin-converting enzyme (ACE) 2 receptor and proteolytic processing of the S
65 precursor into the active S1 and S2 subunits (3–5). However, additional host factors may affect
66 the efficiency of SARS-CoV-2 entry and play roles in viral transmission and pathogenesis (6).

67 We recently demonstrated that interferon-inducible transmembrane proteins (IFITMs 1, 2,
68 and 3) are required for efficient SARS-CoV-2 infection (7). This came as surprise since IFITMs
69 are a family of IFN stimulated genes (ISGs) that are well-known to protect cells against infection
70 by numerous viral pathogens including retro-, flavi-, influenza-, rhabdo-, filo- and bunyaviruses
71 (3–5). Inhibitory effects have also been reported for highly pathogenic coronaviruses, including
72 SARS-CoV-2 (8,9). However, most evidence was obtained using pseudo-particles containing the
73 S protein of SARS or MERS coronaviruses and/or cells that are not intrinsically permissve to
74 this virus, artificially overexpress IFITM proteins and. Notably, it has been reported that the
75 common cold coronavirus OC43 hijacks IFITM3 for efficient entry (10).

76 The antiviral mechanism of IFITMs is thought to involve alterations in the rigidity and
77 curvature of the cellular membrane, affecting viruses in a broad, unspecific way (4, 5, 11). In
78 contrast, the SARS-CoV-2 enhancing effect most likely involves specific interactions between
79 the S protein and the N-terminal region of IFITMs, especially IFITM2 (7), suggesting that this
80 pandemic viral pathogen hijacks IFITMs for efficient infection. In accordance with this knock-
81 down of endogenous IFITM2 expression in human lung cell lines strongly reduced viral entry
82 and infectious virus production. In addition, IFITM2-derived peptides as well as an IFITM2-

83 targeting antibody protected gut organoids and cardiomyocytes against infection and cytopathic
84 effects of SARS-CoV-2 (7).

85 In the initial study, IFITM dependency for efficient infection has only been demonstrated for
86 an early European variant of SARS-CoV-2 isolated in the Netherlands in February 2020 (NL-
87 02-2020) (7). Since then numerous variants have emerged. Some of them show increased
88 transmission fitness and immune evasion and are thus referred to as "variants of concern"
89 (VOCs). Currently, the WHO has categorized five SARS-CoV-2 variants as VOCs: B.1.1.7,
90 B.1.351, P.1, B.1.617.2 and B.1.1.529. The first four, referred to as Alpha, Beta, Gamma and
91 Delta variants, have significantly spread in the human population. The latest (Omicron) variant
92 contains a worrisome number of mutations (12). However, it remains to be seen whether it might
93 outcompete the Delta variant that currently dominates the pandemic and the Omicron variant
94 was not yet Available for biological characterization. Compared to the NL-02-2020 isolate, all
95 VOCs contain various alterations in their S proteins reported to enhance viral infectivity,
96 transmissibility and pathogenicity by affecting ACE2 receptor affinity, proteolytic activation and
97 susceptibility to neutralization (13–15). Here, we examined whether current SARS-CoV-2 VOCs
98 still require IFITM proteins for efficient replication in human lung cells.

99 **RESULTS**

100 To verify that the SARS-CoV-2 VOCs show the expected differences in S compared to the early
101 NL-02-2020 isolate, we performed full-genome sequence analyses of the four variants used for
102 functional analyses. The NL-02-2020 isolate already contains the D614G amino acid substitution
103 within the receptor-binding motif (RBM) which has been reported to increase SARS-CoV-2
104 transmissibility by promoting ACE2 receptor interaction and is also found in all current VOCs
105 (16, 17). As expected, the Spike proteins of the VOCs differed by six to ten amino acid changes
106 from the NL-02-2020 Spike (Figure 1). The Alpha VOC (B.1.1.7) that emerged at the end of
107 2020 in the UK contains eight mutations in its S protein: Deletion of H69/V70 and Y144;

108 Mutation of N501Y, A570D, P681H, T716I, S982A and D1118H (18). The Beta VOC (B.1.351)
109 emerged in South Africa in October 2020 and has initially spread to all continents (19). Its S
110 protein contains three alterations in the RBD (K417N, E484K, N501Y) and five additional
111 changes (L18F, D80A, D215G, R246I, A701V). The Gamma (P.1) variant was first detected in
112 Brazil at the end of 2020 and shares the K417T, E484K and N501Y S mutations with the Alpha
113 and/or Beta VOCs (Figure 1) (20). The Delta (B.1.617.2) variant was first identified in India in
114 the first half of 2021 (21) and has efficiently outcompeted all other SARS-CoV-2 VOCs around
115 the globe. It differs by changes of T19R, deletion of residues 157-158, L452R, T478K, E484K,
116 P681R, R683L and D950N from NL-02-2020 in the S protein (Figure 1). Several changes (L18F,
117 K417T, E484K and N501Y) emerged independently by convergent evolution in several VOCs
118 (14, 22). The reasons why they are associated with a selective advantage remain to be fully
119 elucidated but rapidly accumulating evidence shows they reduce neutralization by antibodies
120 and/or increase ACE2 binding affinity (14). In addition, the P681R substitution near the furin
121 cleavage site might improve proteolytic activation of the Delta S protein (23, 24). Thus, all VOCs
122 contain changes in their S proteins reported to increase interaction with their primary ACE2
123 receptor that might also affect the dependency on other cellular cofactors for efficient entry and
124 fusion, like IFITM proteins.

125 To examine the role of endogenous IFITM expression on infection by genuine SARS-CoV-2
126 VOCs, we performed siRNA knockdown (KD) studies in the human epithelial lung cancer cell
127 line Calu-3, which endogenously express ACE2 and all three IFITM proteins (7). Viral
128 replication was determined by quantification of viral N (nucleocapsid) RNA levels by qRT-PCR
129 in the cell culture supernatants 2 days after infection with the five SARS-CoV-2 variants (Figure
130 2A). Most VOCs produced 2- to 4-fold higher levels of viral RNA compared to NL-02-2020 in
131 Calu-3 cells (Figure 2B). The single exception was the Beta variant, which showed moderately
132 lower levels of viral RNA production. Silencing of IFITM2 expression reduced viral RNA
133 production from 31- (Alpha) to 754-fold (Gamma). Replication of the Beta variant was 112x

134 reduced in the absence of IFITM2, respectively. In comparison, KD of IFITM1 had little effect,
135 while silencing of IFITM3 resulted in 2- (Beta) to a maximum of 31-fold (NL-02-2020) lower
136 viral RNA yields (Figure 2B). Notably, IFITM2 KD still reduced viral RNA yields by the
137 currently dominant Delta variant by >100-fold, while IFITM3 silencing was associated with a
138 20-fold reduction, demonstrating that this VOC still requires IFITM proteins for efficient entry.

139 To further determine whether IFITM2 is critical for productive replication of SARS-CoV-2
140 VOCs in Calu-3 cells, we determined the $TCID_{50}$ (50% Tissue Culture Infectious Dose) of viral
141 particles in the cell culture supernatants (Figure 3A). With the exception of the Beta variant that
142 showed the lowest viral RNA yields (Figure 2) and infectious titers, all SARS-CoV-2 variants
143 produced more than 10 million infectious virus particles per ml culture supernatant in Calu-3
144 cells treated with the control siRNA (Figure 3B). In striking contract, infectious virus production
145 was generally reduced to levels near or below background (≤100 infectious particles per ml)
146 upon silencing of IFITM2 (Figure 3). Altogether, these results show that all four SARS-CoV-2
147 VOCs including the dominant Delta variants are strongly dependent on endogenous IFITM2
148 expression for efficient replication in Calu-3 cells.

149 We have previously shown that an antibody targeting the N-terminus of IFITM2 inhibits
150 replication of the NL-02-2020 isolate in gut organoids and cardiomyocytes (7). To further
151 examine the potential relevance of IFITM2 for transmission of SARS-CoV-2 VOCs, we
152 performed experiments in iPSC-derived alveolar epithelial type II (iATII) cells, as a model for
153 the main target cells of SARS-CoV-2 infection in the distal lung (25). Western blot analyses
154 showed that, similarly to Calu-3 cells, iATII cells express IFITM2 and IFITM3 (Figure 4A). In
155 contrast, both cells types showed little (Calu-3) or no (iATII) detectable expression of IFITM1.
156 Unexpectedly, we did not detect ACE2 expression in iATII cells by western blot analyses while
157 ACE2 was readily detectable in Calu-3 cells (Figure 4A). In agreement with published data (26),
158 however, ACE2 expression by iATII cells was clearly detectable by FACS (Figure 4B).

159 In agreement with published data (26–28), iATII cells were highly susceptible to SARS-CoV-
160 2 replication and typically produced about 100-fold higher levels of viral RNA compared to
161 Calu-3 cells (Figures 2B, 5A). On average, the Delta variant replicated to about 30-fold higher
162 levels (average vRNA copy numbers of $2.4x10^{11}$) than the early NL-02-2020 isolate in iATII
163 cells (Figure 5A). The broad-spectrum antiviral agent Remdesivir (29) efficiently inhibited
164 replication of all SARS-CoV-2 variants. Treatment of iATII cells with the antibody against the
165 N-terminus of IFITM2 also generally reduced viral RNA production in a dose-dependent
166 manner, albeit varying efficiencies. Most notably, the anti-IFITM2 Ab reduced replication of the
167 Delta VOC in iATII cells by up to 95% (Figure 5B). This agrees with our previous finding that
168 IFITM2 can be targeted to protect various types of human cells against SARS-CoV-2 infection
169 (7).

170 **DISCUSSION**

171 In the present study, we demonstrate that IFITMs (especially IFITM2) are also critical cofactors
172 for efficient replication of all four SARS-CoV-2 VOCs including the currently dominant Delta
173 variant. We have previously shown that IFITMs also promote SARS-CoV-2 replication in
174 primary small airway epithelial cells (SAEC) cells and that IFITM2 can be targeted to inhibit
175 viral replication in gut organoids and cardiomyocytes derived from human iPSCs (7). The present
176 finding that an α-IFITM2 antibody inhibits replication of the Delta variants in iPSC-derived
177 alveolar epithelial type II cells, proposed to model main target cells of SARS-CoV-2 infection
178 in the distal lung (26, 28), adds to the evidence that IFITM2 may play a key role in SARS-CoV-
179 2 transmission, dissemination and pathogenesis. Our observation that IFITM2 dependency is
180 maintained by VOCs also further underlines that against the odds this cellular "antiviral" factor
181 represents a target for therapeutic or preventive approaches.

182 In agreement with previous findings (23, 30), the Delta variant replicated with higher
183 efficiency than the early SARS-CoV-2 isolate in human lung cells particularly in iPSC-derived

184 alveolar epithelial type II cells. This agrees with recent data showing that the Delta variant infects
185 human bronchial epithelial cells with higher efficiency than other VOCs (31). Altogether, our
186 results show that IFITMs (especially IFITM2) are also critical cofactors for efficient replication
187 of all four current SARS-CoV-2 VOCs. Notably, however, the Alpha variant yielded ~100-fold
188 higher levels of vRNA upon silencing of IFITM2 expression compared to the 2019 CoV-2 and
189 Beta variants (Figure 2). Thus, it is tempting to speculate that this VOC did not only evolve
190 reduced susceptibility to IFN inhibition (30, 32) but may also dependent less on IFITM2 for
191 efficient infection compared to other SARS-CoV-2 variants.

192 The exact mechanism of IFITM2-dependent enhancement needs further studies. However,
193 our previous studies suggest that IFITM2 promotes SARS-CoV-2 entry by direct interaction with
194 the viral Spike protein and enhancing virus-cell fusion in early endosomes (7). The enhancing
195 effect is only observed for genuine SARS-CoV-2 and endogenous IFITMs, while the broad
196 antiviral activity of IFITMs involving alterations in cellular membrane rigidity and curvature
197 instead of specific interactions with viral glycoproteins has been reported for pseudovirions
198 carrying SARS-CoV-2 Spike proteins and for overexpression of IFITM proteins (8). In
199 agreement with our previous results (7), IFITM2 KD had stronger effects on infectious titers than
200 on viral RNA yields. It remains to be determined whether the presence of IFITM2 has indeed an
201 enhancing effect on the infectiousness of SARS-CoV-2 particles or if the background levels are
202 just higher for viral RNA due to release from or lysis of infected cells.

203 The Alpha and Delta variants contain a mutation P681H/R close to the furin cleavage site that
204 might affect interferon sensitivity, proteolytic activation and fusogenicity of the S protein (33,
205 34). These two VOCs produced the highest levels of viral RNA upon IFITM2 KD and it will be
206 interesting to further examine whether an increased intrinsic fusogenic activity of the Alpha and
207 Delta Spike proteins affects their dependency on IFITM2 for infection.

208 Our results are further evidence that IFITM proteins are critical cofactors for infection of
209 SARS-CoV-2 in primary human target cells. We show that an α-IFITM2 antibody inhibits
210 replication of the Delta VOC in human alveolar epithelial type II cells by >90% (Figure 5B)
211 reported to play a key role in the spread of SARS-CoV-2. This finding further suggests that
212 IFITM2 may be a highly unexpected suitable target for therapeutic approaches against this
213 pandemic viral pathogen. It will be interesting to determine whether the emerging Omicron
214 variant that contains a striking number of about 30 amino acid changes in the Spike protein
215 compared to the Wuhan strain (15, 35) is also dependent on IFITM2 for efficient infection and
216 susceptible to inhibition by α-ITITM2 antibodies.

217 **ACKNOWLEDGMENTS**

218 We thank Daniela Krnavek, Martha Mayer, Kerstin Regensburger, Regina Burger, Jana Romana
219 Fischer and Birgit Ott for laboratory assistance. We also thank Stefan Krebs, Helmut Blum,
220 Alexander Graf for next generation sequencing of SARS-CoV-2 VOCs, Michael Schindler for
221 providing the B.1.351 (Beta) VOC and Florian Schmidt, Beate M. Kümmerer and Hendrick
222 Streeck for providing the B.1.617.2 (Delta) VOC. The following reagent was obtained through
223 BEI Resources, NIAID, NIH: SARS-CoV-2, Isolate hCoV-19/Japan/TY7-503/2021 (Brazil P.1),
224 NR-54982, contributed by National Institute of Infectious Diseases.

225 **FUNDING**

226 This study was supported by DFG grants to F.K. (CRC 1279) and K.M.J.S. (CRC 1279,
227 SP1600/6-1), the BMBF to F.K. and K.M.J.S. (Restrict SARS-CoV-2, and IMMUNOMOD) and
228 a COVID-19 research grant from the Ministry of Science, Research and the Arts of Baden-
229 Württemberg (MWK) to F.K. A.S. and M.F. were supported by the DFG (project numbers
230 278012962 & 458685747). The BU3-NGST iPSC line was generated with funding from the
231 National Center for Advancing Translational Sciences ("NCATS") (grant U01TR001810) and
232 kindly provided by D.N. Kotton (Center for Regenerative Medicine, Boston Medical Center).

233 **AUTHORS INFORMATION**

234 Conceptualization and funding acquisition, F.K., K.M.J.S., M.F.; Investigation, R.N., C.P.B.,
235 F.Z., L.K., D.K. and A. S.; Writing, F.K.; Review and editing, all authors.

236 **COMPETING INTERESTS**

237 The authors declare no competing interests.

238 **MATERIAL AND METHODS**

239 **Cell culture.** Calu-3 (human epithelial lung adenocarcinoma) cells were cultured in Minimum
240 Essential Medium Eagle (MEM, Sigma, Cat#M4655) supplemented with 10% (upon and after
241 viral infection) or 20% (during all other times) heat-inactivated fetal bovine serum (FBS, Gibco,
242 Cat#10270106), 100 units/ml penicillin, 100 µg/ml streptomycin (ThermoFisher,
243 Cat#15140122), 1 mM sodium pyruvate (Pan Biotech, Cat#P04-8010), and 1x non-essential
244 amino acids (Sigma, Cat#M7145). Vero E6 cells (Cercopithecus aethiops derived epithelial
245 kidney, ATCC) and TMPRSS2-expressing Vero E6 cells (kindly provided by the National
246 Institute for Biological Standards and Control (NIBSC), No. 100978) were grown in Dulbecco's
247 modified Eagle's medium (DMEM, Gibco, Cat#41965039) supplemented with 2.5% (upon and
248 after viral infection) or 10% (during all other times) heat-inactivated FBS (Gibco,
249 Cat#10270106), 100 units/ml penicillin, 100 µg/ml streptomycin (ThermoFisher,
250 Cat#15140122), 2 mM L-glutamine (Gibco, Cat#25030081), 1 mM sodium pyruvate (Pan
251 Biotech, Cat# P04-8010), 1x non-essential amino acids (Sigma, Cat#M7145) and 1 mg/mL
252 Geneticin (Gibco, Cat#10131-019) (for TMPRSS2-expressing Vero E6 cells). Caco-2 cells
253 (human epithelial colorectal adenocarcinoma, kindly provided by Prof. Holger Barth (Ulm
254 University)) were grown in the same media as Vero E6 cells but with supplementation of 10%
255 heat-inactivated FBS.

256 Human induced Alveolar Type 2 cells (iATII) were differentiated from BU3 NKX2-
257 1^{GFP};$SFTPC^{tdTomato}$ induced pluripotent stem cells(36) (iPCSs, kindly provided by Darrell

258 Kotton, Boston University and Boston Medical Center) and maintained as alveolospheres
259 embedded in 3D Matrigel in CK+DCI media, as previously described(37). For infection studies,
260 iATII cells were cultured as 2D cultures on Matrigel-coated plates in CK+DCI medium + 10 µM
261 Y-27632 (Tocris, Cat#1254) for 48h before switching to CK+DCI medium on day 3.

262 **SARS-CoV-2 stocks.** The SARS-CoV-2 variant B.1.351 (Beta), 2102-cov-IM-r1-164 was
263 provided by Prof. Michael Schindler (University of Tübingen) and the B.1.617.2 (Delta) variant
264 by Prof. Florian Schmidt (University of Bonn). The BetaCoV/Netherlands/01/NL/2020 (NL-02-
265 2020) and B.1.1.7. (Alpha) variants were obtained from the European Virus Archive. The hCoV-
266 19/Japan/TY7-503/2021 (Brazil P.1) (Gamma) (#NR-54982) isolate was obtained from the BEI
267 resources. SARS-CoV-2 strains were propagated on Vero E6 (NL-02-2020, Delta), VeroE6
268 overexpressing TMPRSS2 (Alpha), CaCo-2 (Beta) or Calu-3 (Gamma) cells. To this end, 70-
269 90% confluent cells in 75 cm^2 cell culture flasks were inoculated with the SARS-CoV-2 isolate
270 (multiplicity of infection (MOI) of 0.03-0.1) in 3.5 ml serum-free medium. The cells were
271 incubated for 2h at 37°C, before adding 20 ml medium containing 15 mM HEPES (Carl Roth,
272 Cat#6763.1). Virus stocks were harvested as soon as strong cytopathic effect (CPE) became
273 apparent. The virus stocks were centrifuged for 5 min at 1,000 g to remove cellular debris,
274 aliquoted, and stored at -80°C until further use.

275 **Sequencing of SARS-CoV-2 VOCs.** Virus stocks were inactivated and lysed by adding 0.3 ml
276 TRIzol Reagent (ambion, Cat#132903) to 0.1 ml virus stock. Viral RNA was isolated using the
277 Direct-zol RNA MiniPrep kit (ZymoResearch, Cat#R2050) according to manufacturer's
278 instructions, eluting the RNA in 50 µl DNase/RNase free water. The protocol to prepare the viral
279 RNA for sequencing was modified from the nCoV-2019 sequencing protocol V.1. For reverse
280 transcription, the SuperScript IV First-Strand Synthesis System (Invitrogen, Cat#18091050) was
281 used with modified manufacturer's instructions. First, 1 µl random hexamers (50 ng/µl), 1 µl
282 dNTPs mix (10 mM each), and 11 µl template RNA (diluted 1:10 in DNase/RNase free water)

283 were mixed, incubated at 65°C for 5 min and placed on ice for 1 min. Next, 4 µl SSIV Buffer, 1
284 µl DTT (100 mM), 1 µl RNaseOUT RNase Inhibitor, and 1 µl SSIV Reverse Transcriptase were
285 added to the mix, followed by incubation at 24°C for 5 min, 42°C for 50 min, and 70°C for 10
286 min. To generate 400 nt fragments in PCR, the ARTIC nCoV-2019 V3 Primer set (IDT) and the
287 Q5 Hot Start High-Fidelity 2X Master Mix (NEB, Cat#M0494S) were used with modified
288 manufacturer's instructions. The primers pools 1 and 2 were diluted to a final concentration of
289 10 µM and a reaction with each primer pool was set up as follows, 4 µl respective primer pool,
290 12.5 µl Q5 Hot Start High-Fidelity 2X Master Mix, 6 µl water, and 2.5 µl cDNA. The PCR was
291 performed as follows, 98°C for 30 s, 30 cycles of 98°C for 15 s and 65°C for 5 min, and hold at
292 4°C. The PCR products were run on a 1% agarose gel to check for the presence of fragments at
293 the correct size. The products from primer pool 1 and primer pool 2 for each variant were pooled,
294 diluted and quantified by Qubit DNA HS kit (Thermo Fisher, Cat#Q32851). The sequencing
295 amplicon pools were diluted to 0.2 ng/µl and tagmented with Nextera XT library prep kit
296 (Illumina, Cat#FC-131-1024). Nextera libraries were dual-barcoded and sequenced on an
297 Illumina NextSeq1000 instrument. The obtained sequenced reads were demultiplexed and
298 mapped against the SARS-CoV-2 reference genome (NC_045512.2) with *BWA-MEM*(38).
299 Pileup files were generated from the mapped reads using *Samtools*(39). The mapped reads and
300 the pileup file were used to construct the consensus sequence with the *iVar* package (40) using
301 default settings.

302 **IFITM knock-down.** At 24 h and 96 h post-seeding, 150,000 Calu-3 cells, seeded in 24-well
303 plates, were transfected with 20 µM of non-targeting siRNA or IFITM1, IFITM2 or IFITM3
304 specific siRNAs using Lipofectamine RNAiMAX (Thermo Fisher, Cat#13778100) according to
305 the manufacturer's instructions. 6 h after the second transfection, Calu-3 cells were infected with
306 the various SARS-CoV-2 variants at an MOI of 0.05. 6 h post-infection, the inoculum was
307 removed, the cells washed once with PBS and supplemented with fresh media. 48 h post
308 infection, supernatants were harvested for qRT-PCR analysis.

309 **qRT-PCR.** *N* (nucleoprotein) transcript levels were determined in supernatants collected from
310 SARS-CoV-2 infected Calu-3 cells 48 h post-infection as previously described(41). Total RNA
311 was isolated using the Viral RNA Mini Kit (Qiagen, Cat#52906) according to the manufacturer's
312 instructions. RT-qPCR was performed as previously described(42) using TaqMan Fast Virus 1-
313 Step Master Mix (Thermo Fisher, Cat#4444436) and a OneStepPlus Real-Time PCR System
314 (96-well format, fast mode). Primers were purchased from Biomers (Ulm, Germany) and
315 dissolved in RNAse free water. Synthetic SARS-CoV-2-RNA (Twist Bioscience, Cat#102024)
316 or RNA isolated from BetaCoV/France/IDF0372/2020 viral stocks quantified via this synthetic
317 RNA (for low Ct samples) were used as a quantitative standard to obtain viral copy numbers. All
318 reactions were run in duplicates. Forward primer (HKU-NF): 5'-TAA TCA GAC AAG GAA
319 CTG ATT A-3'; Reverse primer (HKU-NR): 5'-CGA AGG TGT GAC TTC CAT G-3'; Probe
320 (HKU-NP): 5'-FAM-GCA AAT TGT GCA ATT TGC GG-TAMRA-3'.

321 **Inhibition by IFITM2 antibody and Remdesivir.** 30,000 iATII cells were seeded as single
322 cells in 96-well plates coated for 1 h at 37 °C with 0.16 mg/ml Matrigel (Corning, Cat#356238)
323 diluted in DMEM/F12 (Thermo Fisher, Cat#11330032), 24 h later cells were treated with
324 increasing concentrations (20, 40, 80 µg/ml) of α-IFITM2 (Cell Signaling, Cat#13530 S) or
325 Remdesivir (Selleck Chemicals Cat#S8932) (10 µM). One h post-treatment, cells were infected
326 with SARS-CoV-2 VOCs with a MOI of 0.5. 6 h post-infection, cells were washed once with
327 PBS and supplemented with fresh medium. Thereafter, day 0 wash CTRL was harvested. 48 h
328 post-infection supernatants were harvested for qRT-PCR analysis.

329 **Western blot.** To determine the expression of cellular and viral proteins, infected Calu-3 (MOI
330 0.2, 48 h post infection) or iATII (MOI 0.5, 48 h post infection) cells or uninfected controls were
331 washed in PBS and subsequently lysed in Western blot lysis buffer (150 mM NaCl, 50 mM
332 HEPES, 5 mM EDTA, 0.1% NP40, 500 µM Na3VO4, 500 µM NaF, pH 7.5) supplemented with
333 protease inhibitor cocktail (Roche, Cat#11697498001). After 5 min of incubation on ice, samples

334 were centrifuged (4 °C, 20 min, 20,817 g) to remove cell debris. The supernatant was transferred
335 to a fresh tube, the protein concentration was measured by Nanodrop and adjusted using Western
336 blot lysis buffer. Western blotting was performed as previously reported. Proteins were stained
337 using primary antibodies against IFITM1 (α-IFITM1, Cell Signaling Cat#13126S, 1:1,000),
338 IFITM2 (α-IFITM2 Cell Signaling Cat#13530 S, 1:1,000), IFITM3 (α-IFITM3 Cell Signaling
339 Cat#59212S, 1:1,000), ACE2 (Rabbit polyclonal anti-ACE2 Abcam, Cat#ab166755, 1:1,000);
340 rat anti-GAPDH (Biolegend Cat#607902, 1:1,000) and SARS CoV-2 N (anti-SARS-CoV-2 N
341 Sino Biologicals Cat#40588-V08B, 1:1,000) and Infrared Dye labeled secondary antibodies (LI-
342 COR IRDye). Membranes were scanned using an Odyssey infrared imager and band intensities
343 were quantified in Image Studio Lite Version 5.0.

344 **$TCID_{50}$ Endpoint titration.** 10,000 Caco-2 cells were seeded in 96-well F-bottom plates. One
345 day later, infectious supernatants were serially diluted and added to the cells. Cells were then
346 incubated for 5 days and monitored for CPE. $TCID_{50}$/mL was calculated according to Reed and
347 Muench.

348 **Flow cytometric analysis.** 60,000 iATII cells or Calu-3 cells were incubated for 1 h at 4°C with
349 equal protein concentrations of control rabbit IgG (Diagenode, Cat#C15410206) or 1/200
350 dilution of rabbit anti-ACE2 (Abcam, Cat#ab166755) diluted in FACS buffer (PBS, 1% FBS),
351 washed three times in PBS, stained for 30 min with 1/400 dilution of goat anti-rabbit AF647
352 (Invitrogen, Cat#A27040), fixed in 1% PFA and analyzed using a BD FACS Canto II flow
353 cytometer.

354 **Statistical analysis**

355 Statistical analysis was performed using GraphPad Prism software. Two-tailed unpaired
356 Student's t-test were used to determine statistical significance. Significant differences are
357 indicated as: *, $p < 0.05$; **, $p < 0.01$; ***, $p < 0.001$; **** $p<0.0001$. Statistical parameters are
358 specified in the figure legends.

359 **REFERENCES**

360 1. Zhou P, Yang XL, Wang XG, Hu B, Zhang L, Zhang W, Si HR, Zhu Y, Li B, Huang CL,
361 Chen HD, Chen J, Luo Y, Guo H, Jiang RD, Liu MQ, Chen Y, Shen XR, Wang X, Zheng
362 XS, Zhao K, Chen QJ, Deng F, Liu LL, Yan B, Zhan FX, Wang YY, Xiao GF, Shi ZL. 2020.
363 A pneumonia outbreak associated with a new coronavirus of probable bat origin. Nature
364 579:270–273.

365 2. Zhu N, Zhang D, Wang W, Li X, Yang B, Song J, Zhao X, Huang B, Shi W, Lu R, Niu P,
366 Zhan F, Ma X, Wang D, Xu W, Wu G, Gao GF, Tan W, China Novel Coronavirus
367 Investigating and Research Team. 2020. A Novel Coronavirus from Patients with Pneumonia
368 in China, 2019. N Engl J Med 382:727–733.

369 3. Bailey CC, Zhong G, Huang I-C, Farzan M. 2014. IFITM-Family Proteins: The Cell's First
370 Line of Antiviral Defense. Annual Review of Virology 1:261–283.

371 4. Diamond MS, Farzan M. 2013. The broad-spectrum antiviral functions of IFIT and IFITM
372 proteinsNature Reviews Immunology. Nature Publishing Group.

373 5. Zhao X, Li J, Winkler CA, An P, Guo JT. 2019. IFITM genes, variants, and their roles in the
374 control and pathogenesis of viral infectionsFrontiers in Microbiology. Frontiers Media S.A.

375 6. Baggen J, Vanstreels E, Jansen S, Daelemans D. 2021. Cellular host factors for SARS-CoV-
376 2 infection. Nat Microbiol 6:1219–1232.

377 7. Prelli Bozzo C, Nchioua R, Volcic M, Koepke L, Krüger J, Schütz D, Heller S, Stürzel CM,
378 Kmiec D, Conzelmann C, Müller J, Zech F, Braun E, Groß R, Wettstein L, Weil T, Weiß J,
379 Diofano F, Rodríguez Alfonso AA, Wiese S, Sauter D, Münch J, Goffinet C, Catanese A,
380 Schön M, Boeckers TM, Stenger S, Sato K, Just S, Kleger A, Sparrer KMJ, Kirchhoff F.

381 2021. IFITM proteins promote SARS-CoV-2 infection and are targets for virus inhibition in
382 vitro. Nat Commun 12:4584.

383 8. Shi G, Kenney AD, Kudryashova E, Zani A, Zhang L, Lai KK, Hall-Stoodley L, Robinson
384 RT, Kudryashov DS, Compton AA, Yount JS. 2020. Opposing activities of IFITM proteins
385 in SARS-CoV-2 infection. EMBO J e106501.

386 9. Wrensch F, Winkler M, Pöhlmann S. 2014. IFITM proteins inhibit entry driven by the
387 MERS-Coronavirus Spike protein: Evidence for Cholesterol-Independent Mechanisms.
388 Viruses 6:3683–3698.

389 10. Zhao X, Guo F, Liu F, Cuconati A, Chang J, Block TM, Guo JT. 2014. Interferon induction
390 of IFITM proteins promotes infection by human coronavirus OC43. Proceedings of the
391 National Academy of Sciences of the United States of America 111:6756–6761.

392 11. Compton AA, Bruel T, Porrot F, Mallet A, Sachse M, Euvrard M, Liang C, Casartelli N,
393 Schwartz O. 2014. IFITM proteins incorporated into HIV-1 virions impair viral fusion and
394 spread. Cell Host and Microbe 16:736–747.

395 12. Classification of Omicron (B.1.1.529): SARS-CoV-2 Variant of Concern.

396 13. Soh SM, Kim Y, Kim C, Jang US, Lee H-R. 2021. The rapid adaptation of SARS-CoV-2-
397 rise of the variants: transmission and resistance. J Microbiol 59:807–818.

398 14. Harvey WT, Carabelli AM, Jackson B, Gupta RK, Thomson EC, Harrison EM, Ludden C,
399 Reeve R, Rambaut A, COVID-19 Genomics UK (COG-UK) Consortium, Peacock SJ,
400 Robertson DL. 2021. SARS-CoV-2 variants, spike mutations and immune escape. Nat Rev
401 Microbiol 19:409–424.

402 15. Genovese L, Zaccaria M, Farzan M, Johnson WE, Momeni B. 2021. Investigating the
403 mutational landscape of the SARS-CoV-2 Omicron variant via ab initio quantum mechanical
404 modeling.

405 16. Korber B, Fischer WM, Gnanakaran S, Yoon H, Theiler J, Abfalterer W, Hengartner N,
406 Giorgi EE, Bhattacharya T, Foley B, Hastie KM, Parker MD, Partridge DG, Evans CM,
407 Freeman TM, de Silva TI, Sheffield COVID-19 Genomics Group, McDanal C, Perez LG,
408 Tang H, Moon-Walker A, Whelan SP, LaBranche CC, Saphire EO, Montefiori DC. 2020.
409 Tracking Changes in SARS-CoV-2 Spike: Evidence that D614G Increases Infectivity of the
410 COVID-19 Virus. Cell 182:812-827.e19.

411 17. Yurkovetskiy L, Wang X, Pascal KE, Tomkins-Tinch C, Nyalile TP, Wang Y, Baum A,
412 Diehl WE, Dauphin A, Carbone C, Veinotte K, Egri SB, Schaffner SF, Lemieux JE, Munro
413 JB, Rafique A, Barve A, Sabeti PC, Kyratsous CA, Dudkina NV, Shen K, Luban J. 2020.
414 Structural and Functional Analysis of the D614G SARS-CoV-2 Spike Protein Variant. Cell
415 183:739-751.e8.

416 18. Borges V, Sousa C, Menezes L, Gonçalves AM, Picão M, Almeida JP, Vieita M, Santos R,
417 Silva AR, Costa M, Carneiro L, Casaca P, Pinto-Leite P, Peralta-Santos A, Isidro J, Duarte
418 S, Vieira L, Guiomar R, Silva S, Nunes B, Gomes JP. 2021. Tracking SARS-CoV-2 lineage
419 B.1.1.7 dissemination: insights from nationwide spike gene target failure (SGTF) and spike
420 gene late detection (SGTL) data, Portugal, week 49 2020 to week 3 2021. Euro Surveill 26.

421 19. Tegally H, Wilkinson E, Giovanetti M, Iranzadeh A, Fonseca V, Giandhari J, Doolabh D,
422 Pillay S, San EJ, Msomi N, Mlisana K, von Gottberg A, Walaza S, Allam M, Ismail A,
423 Mohale T, Glass AJ, Engelbrecht S, Van Zyl G, Preiser W, Petruccione F, Sigal A, Hardie
424 D, Marais G, Hsiao N-Y, Korsman S, Davies M-A, Tyers L, Mudau I, York D, Maslo C,
425 Goedhals D, Abrahams S, Laguda-Akingba O, Alisoltani-Dehkordi A, Godzik A, Wibmer

426 CK, Sewell BT, Lourenço J, Alcantara LCJ, Kosakovsky Pond SL, Weaver S, Martin D,
427 Lessells RJ, Bhiman JN, Williamson C, de Oliveira T. 2021. Detection of a SARS-CoV-2
428 variant of concern in South Africa. Nature 592:438–443.

429 20. Faria NR, Mellan TA, Whittaker C, Claro IM, Candido D da S, Mishra S, Crispim MAE,
430 Sales FCS, Hawryluk I, McCrone JT, Hulswit RJG, Franco LAM, Ramundo MS, de Jesus
431 JG, Andrade PS, Coletti TM, Ferreira GM, Silva CAM, Manuli ER, Pereira RHM, Peixoto
432 PS, Kraemer MUG, Gaburo N, Camilo C da C, Hoeltgebaum H, Souza WM, Rocha EC, de
433 Souza LM, de Pinho MC, Araujo LJT, Malta FSV, de Lima AB, Silva J do P, Zauli DAG,
434 Ferreira AC de S, Schnekenberg RP, Laydon DJ, Walker PGT, Schlüter HM, Dos Santos
435 ALP, Vidal MS, Del Caro VS, Filho RMF, Dos Santos HM, Aguiar RS, Proença-Modena
436 JL, Nelson B, Hay JA, Monod M, Miscouridou X, Coupland H, Sonabend R, Vollmer M,
437 Gandy A, Prete CA, Nascimento VH, Suchard MA, Bowden TA, Pond SLK, Wu C-H,
438 Ratmann O, Ferguson NM, Dye C, Loman NJ, Lemey P, Rambaut A, Fraiji NA, Carvalho
439 M do PSS, Pybus OG, Flaxman S, Bhatt S, Sabino EC. 2021. Genomics and epidemiology
440 of the P.1 SARS-CoV-2 lineage in Manaus, Brazil. Science 372:815–821.

441 21. Sheikh A, McMenamin J, Taylor B, Robertson C, Public Health Scotland and the EAVE II
442 Collaborators. 2021. SARS-CoV-2 Delta VOC in Scotland: demographics, risk of hospital
443 admission, and vaccine effectiveness. Lancet 397:2461–2462.

444 22. Martin DP, Weaver S, Tegally H, San JE, Shank SD, Wilkinson E, Lucaci AG, Giandhari J,
445 Naidoo S, Pillay Y, Singh L, Lessells RJ, Gupta RK, Wertheim JO, Nekturenko A, Murrell
446 B, Harkins GW, Lemey P, MacLean OA, Robertson DL, de Oliveira T, Kosakovsky Pond
447 SL. 2021. The emergence and ongoing convergent evolution of the SARS-CoV-2 N501Y
448 lineages. Cell 184:5189-5200.e7.

449 23. Mlcochova P, Kemp SA, Dhar MS, Papa G, Meng B, Ferreira IATM, Datir R, Collier DA,
450 Albecka A, Singh S, Pandey R, Brown J, Zhou J, Goonawardane N, Mishra S, Whittaker C,
451 Mellan T, Marwal R, Datta M, Sengupta S, Ponnusamy K, Radhakrishnan VS, Abdullahi A,
452 Charles O, Chattopadhyay P, Devi P, Caputo D, Peacock T, Wattal C, Goel N, Satwik A,
453 Vaishya R, Agarwal M, Indian SARS-CoV-2 Genomics Consortium (INSACOG), Genotype
454 to Phenotype Japan (G2P-Japan) Consortium, CITIID-NIHR BioResource COVID-19
455 Collaboration, Mavousian A, Lee JH, Bassi J, Silacci-Fegni C, Saliba C, Pinto D, Irie T,
456 Yoshida I, Hamilton WL, Sato K, Bhatt S, Flaxman S, James LC, Corti D, Piccoli L, Barclay
457 WS, Rakshit P, Agrawal A, Gupta RK. 2021. SARS-CoV-2 B.1.617.2 Delta variant
458 replication and immune evasion. Nature 599:114–119.

459 24. Cherian S, Potdar V, Jadhav S, Yadav P, Gupta N, Das M, Rakshit P, Singh S, Abraham P,
460 Panda S, Team N. 2021. SARS-CoV-2 Spike Mutations, L452R, T478K, E484Q and P681R,
461 in the Second Wave of COVID-19 in Maharashtra, India. Microorganisms 9:1542.

462 25. Delorey TM, Ziegler CGK, Heimberg G, Normand R, Yang Y, Segerstolpe Å, Abbondanza
463 D, Fleming SJ, Subramanian A, Montoro DT, Jagadeesh KA, Dey KK, Sen P, Slyper M,
464 Pita-Juárez YH, Phillips D, Biermann J, Bloom-Ackermann Z, Barkas N, Ganna A, Gomez
465 J, Melms JC, Katsyv I, Normandin E, Naderi P, Popov YV, Raju SS, Niezen S, Tsai LT-Y,
466 Siddle KJ, Sud M, Tran VM, Vellarikkal SK, Wang Y, Amir-Zilberstein L, Atri DS,
467 Beechem J, Brook OR, Chen J, Divakar P, Dorceus P, Engreitz JM, Essene A, Fitzgerald
468 DM, Fropf R, Gazal S, Gould J, Grzyb J, Harvey T, Hecht J, Hether T, Jané-Valbuena J,
469 Leney-Greene M, Ma H, McCabe C, McLoughlin DE, Miller EM, Muus C, Niemi M, Padera
470 R, Pan L, Pant D, Pe'er C, Pfiffner-Borges J, Pinto CJ, Plaisted J, Reeves J, Ross M, Rudy
471 M, Rueckert EH, Siciliano M, Sturm A, Todres E, Waghray A, Warren S, Zhang S, Zollinger
472 DR, Cosimi L, Gupta RM, Hacohen N, Hibshoosh H, Hide W, Price AL, Rajagopal J, Tata
473 PR, Riedel S, Szabo G, Tickle TL, Ellinor PT, Hung D, Sabeti PC, Novak R, Rogers R,

474 Ingber DE, Jiang ZG, Juric D, Babadi M, Farhi SL, Izar B, Stone JR, Vlachos IS, Solomon
475 IH, Ashenberg O, Porter CBM, Li B, Shalek AK, Villani A-C, Rozenblatt-Rosen O, Regev
476 A. 2021. COVID-19 tissue atlases reveal SARS-CoV-2 pathology and cellular targets.
477 Nature 595:107–113.

478 26. Huang J, Hume AJ, Abo KM, Werder RB, Villacorta-Martin C, Alysandratos K-D,
479 Beermann ML, Simone-Roach C, Lindstrom-Vautrin J, Olejnik J, Suder EL, Bullitt E, Hinds
480 A, Sharma A, Bosmann M, Wang R, Hawkins F, Burks EJ, Saeed M, Wilson AA,
481 Mühlberger E, Kotton DN. 2020. SARS-CoV-2 Infection of Pluripotent Stem Cell-Derived
482 Human Lung Alveolar Type 2 Cells Elicits a Rapid Epithelial-Intrinsic Inflammatory
483 Response. Cell Stem Cell 27:962-973.e7.

484 27. van der Vaart J, Lamers MM, Haagmans BL, Clevers H. 2021. Advancing lung organoids
485 for COVID-19 research. Dis Model Mech 14:dmm049060.

486 28. Abo KM, Ma L, Matte T, Huang J, Alysandratos KD, Werder RB, Mithal A, Beermann ML,
487 Lindstrom-Vautrin J, Mostoslavsky G, Ikonomou L, Kotton DN, Hawkins F, Wilson A,
488 Villacorta-Martin C. 2020. Human iPSC-derived alveolar and airway epithelial cells can be
489 cultured at air-liquid interface and express SARS-CoV-2 host factors. bioRxiv
490 2020.06.03.132639.

491 29. Krüger J, Groß R, Conzelmann C, Müller JA, Koepke L, Sparrer KMJ, Schütz D, Seufferlein
492 T, Barth TFE, Stenger S, Heller S, Kleger A, Münch J. 2020. Remdesivir but not famotidine
493 inhibits SARS-CoV-2 replication in human pluripotent stem cell-derived intestinal
494 organoids. bioRxiv 2020.06.10.144816.

495 30. Nchioua R, Schundner A, Klute S, Noettger S, Zech F, Koepke L, Graf A, Krebs S, Blum H,
496 Kmiec D, Frick M, Kirchhoff F, Sparrer KMJ. 2021. The Delta variant of SARS-CoV-2
497 maintains high sensitivity to interferons in human lung cells.

498 31. Li H, Liu T, Wang L, Wang M, Wang S. SARS-CoV-2 Delta variant infects ACE2low
499 primary human bronchial epithelial cells more efficiently than other variants. Journal of
500 Medical Virology n/a.

501 32. Thorne LG, Bouhaddou M, Reuschl A-K, Zuliani-Alvarez L, Polacco B, Pelin A, Batra J,
502 Whelan MVX, Ummadi M, Rojc A, Turner J, Obernier K, Braberg H, Soucheray M,
503 Richards A, Chen K-H, Harjai B, Memon D, Hosmillo M, Hiatt J, Jahun A, Goodfellow IG,
504 Fabius JM, Shokat K, Jura N, Verba K, Noursadeghi M, Beltrao P, Swaney DL, Garcia-
505 Sastre A, Jolly C, Towers GJ, Krogan NJ. 2021. Evolution of enhanced innate immune
506 evasion by the SARS-CoV-2 B.1.1.7 UK variant.

507 33. Peacock TP, Sheppard CM, Brown JC, Goonawardane N, Zhou J, Whiteley M, Consortium
508 PV, Silva TI de, Barclay WS. 2021. The SARS-CoV-2 variants associated with infections in
509 India, B.1.617, show enhanced spike cleavage by furin.

510 34. Liu Y, Liu J, Johnson BA, Xia H, Ku Z, Schindewolf C, Widen SG, An Z, Weaver SC,
511 Menachery VD, Xie X, Shi P-Y. 2021. Delta spike P681R mutation enhances SARS-CoV-2
512 fitness over Alpha variant. bioRxiv 2021.08.12.456173.

513 35. Kumar S, Thambiraja TS, Karuppanan K, Subramaniam G. 2021. Omicron and Delta Variant
514 of SARS-CoV-2: A Comparative Computational Study of Spike protein.

515 36. Jacob A, Morley M, Hawkins F, McCauley KB, Jean JC, Heins H, Na C-L, Weaver TE,
516 Vedaie M, Hurley K, Hinds A, Russo SJ, Kook S, Zacharias W, Ochs M, Traber K, Quinton
517 LJ, Crane A, Davis BR, White FV, Wambach J, Whitsett JA, Cole FS, Morrisey EE,
518 Guttentag SH, Beers MF, Kotton DN. 2017. Differentiation of Human Pluripotent Stem Cells
519 into Functional Lung Alveolar Epithelial Cells. Cell Stem Cell 21:472-488.e10.

520 37. Jacob A, Vedaie M, Roberts DA, Thomas DC, Villacorta-Martin C, Alysandratos K-D,
521 Hawkins F, Kotton DN. 2019. Derivation of self-renewing lung alveolar epithelial type II
522 cells from human pluripotent stem cells. Nat Protoc 14:3303–3332.

523 38. Li H. 2013. Aligning sequence reads, clone sequences and assembly contigs with BWA-
524 MEM. arXiv:13033997 [q-bio].

525 39. Li H, Handsaker B, Wysoker A, Fennell T, Ruan J, Homer N, Marth G, Abecasis G, Durbin
526 R, 1000 Genome Project Data Processing Subgroup. 2009. The Sequence Alignment/Map
527 format and SAMtools. Bioinformatics 25:2078–2079.

528 40. Grubaugh ND, Gangavarapu K, Quick J, Matteson NL, De Jesus JG, Main BJ, Tan AL, Paul
529 LM, Brackney DE, Grewal S, Gurfield N, Van Rompay KKA, Isern S, Michael SF, Coffey
530 LL, Loman NJ, Andersen KG. 2019. An amplicon-based sequencing framework for
531 accurately measuring intrahost virus diversity using PrimalSeq and iVar. Genome Biology
532 20:8.

533 41. Nchioua R, Kmiec D, Müller JA, Conzelmann C, Groß R, Swanson CM, Neil SJD, Stenger
534 S, Sauter D, Münch J, Sparrer KMJ, Kirchhoff F. 2020. SARS-CoV-2 Is Restricted by Zinc
535 Finger Antiviral Protein despite Preadaptation to the Low-CpG Environment in Humans.
536 mBio 11:16.

537 42. Groß R, Conzelmann C, Müller JA, Stenger S, Steinhart K, Kirchhoff F, Münch J. 2020.
538 Detection of SARS-CoV-2 in human breastmilk. The Lancet https://doi.org/10.1016/S0140-
539 6736(20)31181-8.

540

541

542 **Figure legends**

543 **Figure 1: Amino acid variations in the Spike proteins of SARS-CoV-2 variants investigated.**
544 The upper panel shows a schematic representation of the SARS-CoV-2 S protein with specific
545 domains indicated in different colours. Abbreviations: SS, signal sequence; NTD, N-terminal
546 domain; RBD, receptor binding domain; FP, fusion peptide; HR, heptad repeat and TMD,
547 transmembrane domain. The S1/S2 and S2' proteolytic cleavage sites are also indicated.

548

549 **Figure 2: Role of IFITMs in replication of SARS-CoV-2 VOCs in Calu-3 cells.** (**A**) Standard
550 curve and raw qRT-PCR CT values obtained using supernatants of Calu-3 cells collected 2 days
551 post-infection. (**B**) Viral N RNA levels in the supernatant of Calu-3 cells infected with the
552 indicates SARS-CoV-2 variants. Cells were transfected with control (CTRL) or IFITM targeting
553 siRNAs as indicated. Numbers above the bars indicate n-fold reduction compared to the viral
554 RNA levels detected in the supernatant of Calu-3 cells treated with CTRL siRNA. Bars in panel
555 A and B represent the mean of 3 to 4 independent experiments (±SEM) each measured in
556 technical duplicates.

557 **Figure 3: Silencing of endogenous IFITM2 expression prevents production of infectious**
558 **SARS-CoV-2.** (**A**) Supernatants derived from Calu-3 cells treated with control (CTRL) or
559 IFITM2 siRNA two days after infection with the SARS-CoV-2 NL-02-2020 or the indicated
560 VOCs were serially diluted and added to Caco-2 cells seeded in 96-well plates. Five days later,
561 cells were examined for CPE, fixed and stained with crystal violet. Productively infected wells
562 appear transparent since the cells are eliminated or detached due to viral infection. (**B**)
563 Quantification of infectious SARS-CoV-2 particles in the supernatant of Calu-3 cells treated with
564 control or IFITM2 targeting siRNAs. Bars represent the mean of one experiment performed with
565 eight technical replicates (±SD) shown in panel A. Bdl, below detection limit.

566 **Figure 4: Expression of ACE2 and IFITM proteins in Calu-3 and iATII cells.** (**A**)
567 Immunoblot of ACE2, IFITM1, IFITM2, and IFITM3 in Calu-3 and iATII cells left uninfected
568 (c) or infected with the indicated SARS-CoV-2 variants. Whole-cell lysates were stained with
569 the indicated antibodies. An unspecific signal was observed in the Calu-3 control lane stained
570 with the CoV-2 N antibody. (**B**) Flow cytometric analysis of surface ACE2 expression in Calu-
571 3 and iATII cells.

572 **Figure 5: Effect of an α-IFITM2 antibody on replication of SARS-CoV-2 variants in iATII**
573 **cells.** (**A**) Quantification of viral N RNA levels in the supernatant of iATII cells treated with α-
574 IFITM2 antibody (20, 40, or 80 μg/ml) or Remdesivir (10 μM) 1 h before infection (SARS-CoV-
575 2, MOI 0.5), collected 48 h post-infection. Bars represent the mean of three independent
576 experiments. (**B**) Average percentage of reduction of vRNA levels in the supernatants of (E)
577 compared to the untreated control.

Fig. 1 Nchioua et al.,

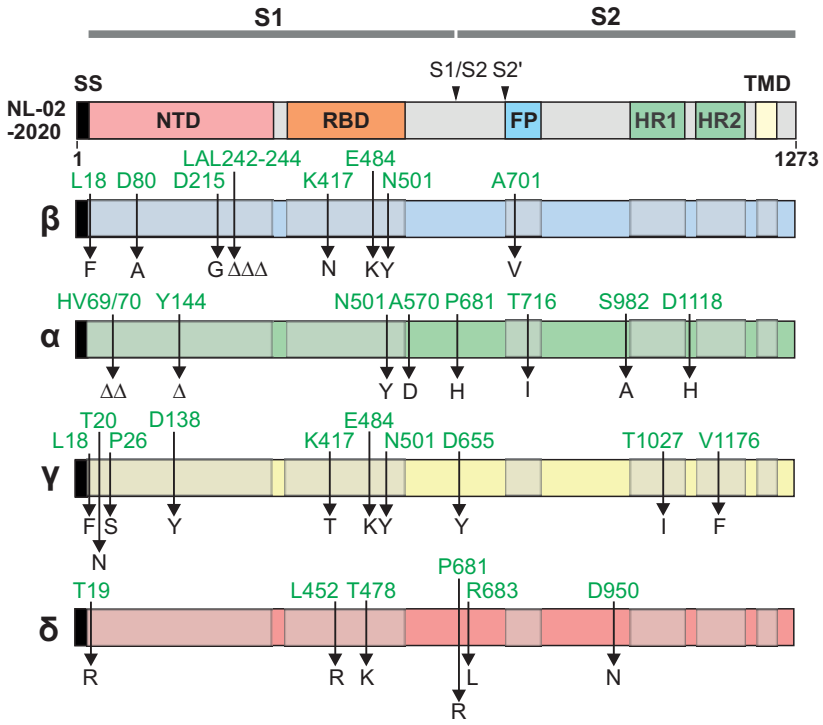

Fig. 2 Nchioua et al.,

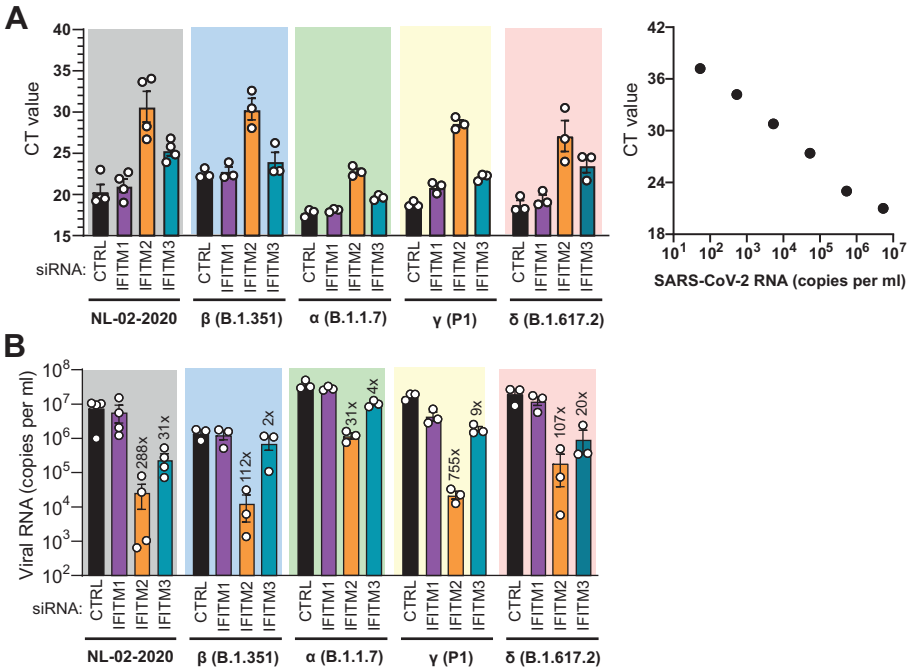

Fig. 3 Nchioua et al.,

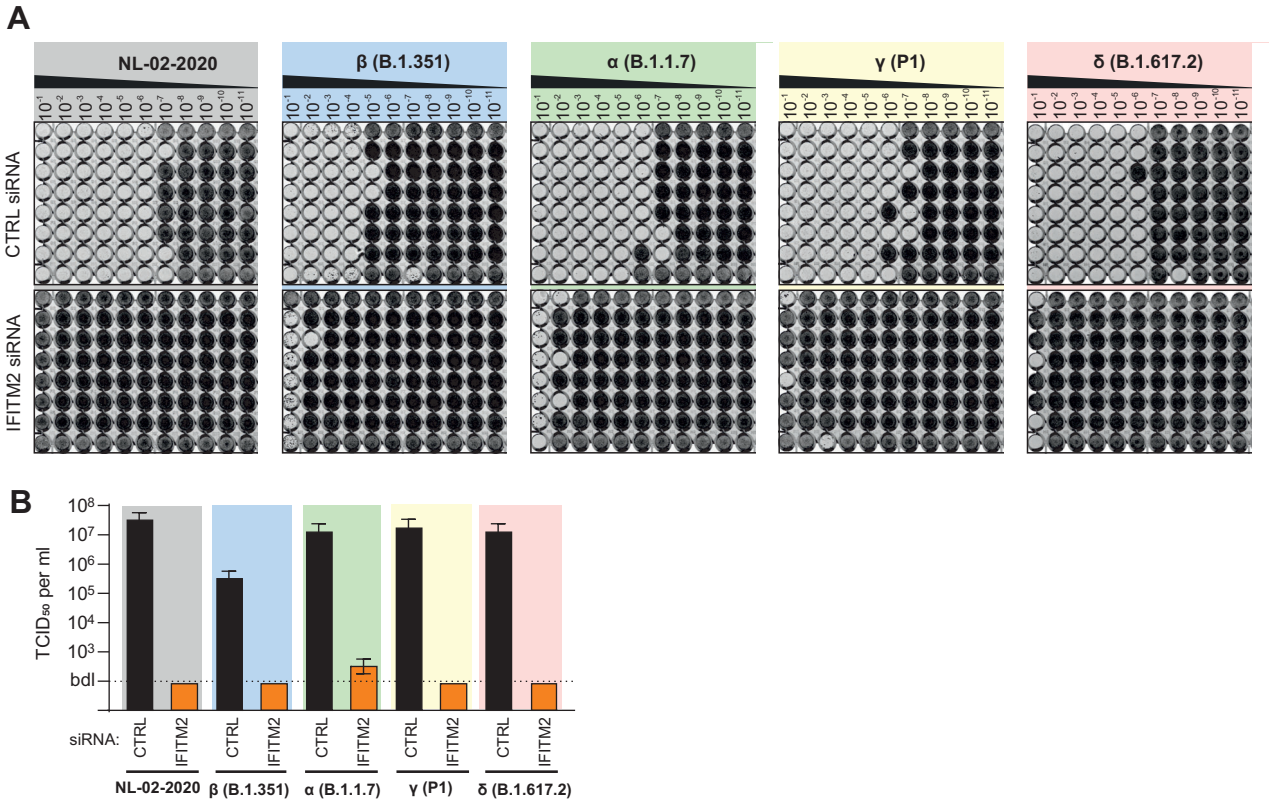

Fig. 2 Nchioua et al.,

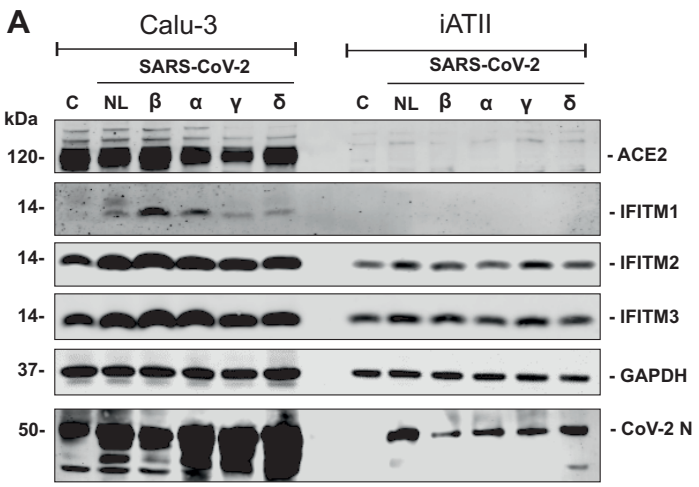

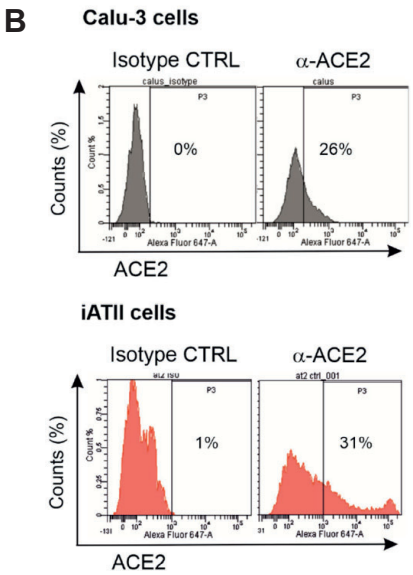
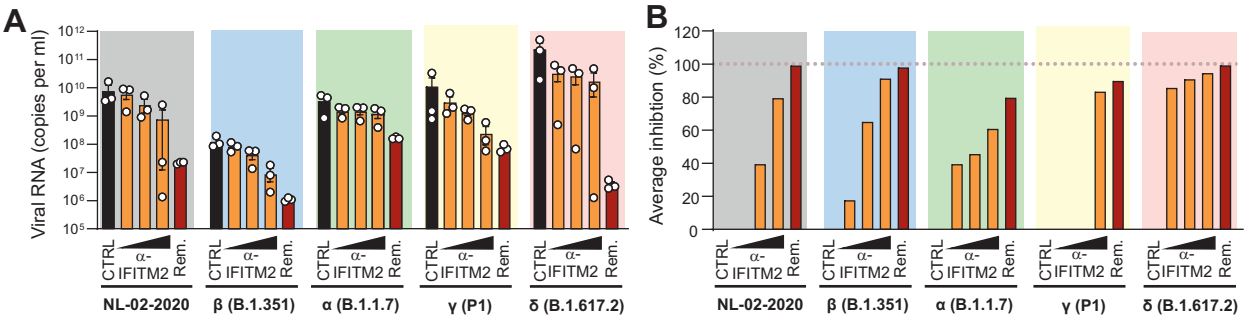
Fig. 5 Nchioua et al.,